Highly Water-Selective Mixed Matrix Membranes from Natural Rubber-*blend*-poly(acrylic acid) (NR-*blend*-PAA) Incorporated with Zeolite 4A for the Dehydration of Water–Ethanol Mixtures through Pervaporation

S. Amnuaypanich,[1] T. Naowanon,[1] W. Wongthep,[1] P. Phinyocheep[2]

[1]*Applied Chemistry Division, Department of Chemistry and Center for Innovation in Chemistry, Faculty of Science, Khon Kaen University, Khon Kaen 40002, Thailand*
[2]*Department of Chemistry, Faculty of Science, Mahidol University, Bangkok 10400, Thailand*

Received 20 August 2010; accepted 19 April 2011
DOI 10.1002/app.34722
Published online 2 February 2012 in Wiley Online Library (wileyonlinelibrary.com).

ABSTRACT: The mixed matrix membranes (MMMs) were developed from a composite of hydrophobic-hydrophilic NR-*blend*-PAA with zeolite 4A. A separation performance of the MMMs was investigated by performing the pervaporation dehydration of water–ethanol mixtures. The results showed a dramatically greater flux of water than the ethanol flux indicating that the developed membranes were highly water-selective. Upon incorporating of zeolite 4A, the flux and separation factor were significantly improved. Increasing the water content in the water–ethanol feed mixtures resulted in an increase in both water and ethanol fluxes leading to a decrease in water separation factor. Similarly a flux-separation factor trade-off was observed as raising feed temperature. The water permeance, however, declined when either the feed water concentration or the feed temperature increased. This suggests that the driving force, i.e. the partial pressure difference, has a pronounced effect on the water flux enhancement. Conversely, the driving force was less influential on the ethanol permeance. The activation energies of the permeations obtained from the Arrhenius plots, showed the lower activation energies of water permeation than those of ethanol permeation; this is because water molecules experiences less restrictive passage through the membranes compared with ethanol molecules. © 2012 Wiley Periodicals, Inc. J Appl Polym Sci 124: E319–E329, 2012

Key words: pervaporation; natural rubber; poly(acrylic acid); zeolite 4A; mixed matrix membrane

INTRODUCTION

Alternative energies gain considerably attention over the last decade due to increasing fuel consumption while petroleum reserves are being depleted. One of these alternative fuel sources is ethanol particularly when blended with gasoline to use as automotive fuel. To be compatible with gasoline, ethanol must have a water content of less than 1.0 vol %.[1] To meet such specification, other methods of separation, rather than the conventional distillation method, are needed because ethanol forms an azeotropic mixture with water at 96.0 wt %.[2] One process capable of braking of azeotropes is the pervaporation. As a membrane-based process, the pervaporation separates liquid mixtures by differences in the solubility and the diffusivity of each component with the membrane. In addition, without the use of heat to generate a phase change during separation, the pervaporation is also suitable for close boiling point components and heat-sensitive mixtures.

To achieve a good separation in the membrane-based separation, the membranes must possess both high permeability as well as selectivity and those qualities are strongly dependent on the characteristics of the materials used for fabricating a membrane. In a dehydration process using the polymeric membranes, the membranes normally consist of polymers with water-attractive functional groups in order to make them water-preferential.[3] With the presence of carboxylic acid groups, poly(acrylic acid) (PAA) is very hydrophilic thus it could be exploited as the water-selective membrane. However, without proper modifications being applied, the PAA membrane suffers from extensive swelling. This is especially true when it is employed under high water content in feed mixtures due to increasing interactions between water molecules and PAA functional groups. Inevitably, the water selectivity of a membrane deteriorates and in

Correspondence to: S. Amnuaypanich (asitti@kku.ac.th).
Contract grant sponsor: Commission on Higher Education, Ministry of Education and Thailand Research Fund (TRF); contract grant number: MRG5180289.
Contract grant sponsor: Center for Innovation in Chemistry (PERCH-CIC), Commission on Higher Education, Ministry of Education, Thailand.
Contract grant sponsor: The Higher Education Research Promotion and National Research University Project of Thailand, Office of the Higher Education Commission through the Biofuel Cluster of Khon Kaen University.

most cases leads to losses of the membranes' integrity. Therefore in preparing the membranes, PAA must be crosslinked either chemically with crosslink agents[4-6] or physically via ionic-interactions with polycations.[7-9] Another method to limit the membrane swelling is blending a hydrophilic polymer with a hydrophobic one.[10,11] The hydrophilic-hydrophobic blend membranes have been found to improve the water separation factor in the pervaporation dehydration of water–ethanol mixtures.[12]

Unfortunately, due to the dense structure of polymeric membranes, the water selectivity is enhanced with a decline of the water permeation flux or vice versa.[13] To alleviate this trade-off; that is the water flux across the membrane could be increased without sacrifice of the membrane selectivity, one approach is to incorporate well-defined structure particles e.g., zeolites NaA or 4A with the polymer matrix to produce the mixed matrix membranes (MMMs).[14,15] The porous structure of zeolites provides additional diffusing paths for the membrane-favored permeant and the zeolites' micropores in the range of 3–10 °A can separate permeants based on shape and size difference.[16] Moreover, zeolites are resistant to most polar and nonpolar solvents because of their rigid crystalline structures therefore when incorporating into the polymer matrix, the membrane swelling is reduced. Huang et al.[14] investigated the pervaporation dehydration of water–ethanol mixtures using MMMs from crosslinked PVA incorporated with zeolite 4A. The pervaporation results showed that the total permeation and the water separation factor were improved upon adding the zeolite, mainly due to the molecular sieving effect of the incorporated zeolite. Guan et al.[15] developed the multilayer MMMs consisting of the zeolite 3A-filled PVA selective layer, the porous poly(acrylonitrile-*co*-methyl acrylate) intermediate layer and the polyphenylene sulfide nonwoven fabrics substrate. The pervaporation dehydration of water–ethanol mixtures revealed that the separation performance of the developed MMM was superior to that of multilayer membranes without zeolite. Additionally, the activation energy of the water permeation of the MMM was lower than that of the dense membrane indicating that in transport through the MMM, water molecules experience a less energy barrier from the hydrophilic channels of zeolite. Qiao et al.[17] prepared the MMMs from P84 copolyimide embedded with two different zeolites, i.e., 5A and 13X. The results of the pervaporation dehydration of isopropanol showed that 13X incorporated P84 membrane had a much higher permeability than the membrane filled with zeolite 5A. This was because zeolite 13X possesses bigger pore size, larger pore volume and higher sorption capacity compared with zeolite 5A. Fu et al.[18] observed the similar results in the pervaporation separation of water–ethanol mixtures using the polysulfone membrane filled with zeolites 4A and 13X.

In this study, the concepts of swelling-controlled hydrophilic-hydrophobic polymer blend and enhanced water permeation zeolite-filled membrane are combined to develop the new mixed matrix membranes for the dehydration of water–ethanol mixtures by means of the pervaporation. The MMMs were prepared from polymeric blend of natural rubber (NR) and poly(acrylic acid) (PAA) composited with the zeolite 4A. The PAA provides the water-attractive sites for the membrane thus water absorption is promoting whilst the hydrophobic nature of NR limits the penetration of water molecules into the membrane hence suppressing an excessive membrane swelling. Moreover, NR is an elastomer with very low glass-transition temperature and is available in latex form which readily allow the fabrication of thin film with no require of organic solvent. The zeolite 4A is added to enhance the water permeation also, with a pore size smaller than the molecular size of ethanol but larger than that of water,[19] the zeolite offers a molecular sieving such that water molecules are allowed to pass through the membrane while ethanol molecules are being excluded.

EXPERIMENTAL

Materials

NR latex with ~ 60 wt % dry rubber content was purchased from Thai Hua Rubber Co. Ltd. (Udonthani, Thailand). The latex was centrifuged at 10,000 rpm for 20 min to remove nonrubber components. Appeared as an upper cream-layer in the centrifuge tube, the concentrated NR was carefully removed and redispersed in 7 wt % NH_4OH. The centrifugation-redispersion cleaning process was performed twice. PAA with M_w ~ 1,250,000 g/mol and zeolite 4A with a particle size of 1–2 μm were supplied by Sigma-Aldrich (St. Louis, USA). The zeolite was heated at 300°C for 24 h to remove water trapped in the zeolite pores before stored in a desiccator for further use. Ethylene glycol (EG) was used as the crosslink agent for PAA and was obtained from Carlo Erba Reagenti (Milan, Italy). AR grade absolute Ethanol (99.9 vol %) was supplied by Merck Chemicals (Darmstadt, Germany). Water used in the experiments was distilled and deionized (DI).

Membrane preparation

The MMMs were prepared as follows. Dry PAA was dissolved in 30 wt % NH_4OH. After obtaining complete solution of PAA, zeolite 4A was added and the mixture was stirred rigorously using a mechanical stirrer. Next the NR latex was mixed with the

TABLE I
Weight Composition of Materials for Preparation of NR/PAA and MMMs

Membrane	Weight ratio of NR : PAA	Weight ratio of NR/PAA10 : zeolite 4A	NR (g, dry weight)	PAA (g)	Zeolite 4A (g)
NR/PAA10	90 : 10	–	6.0	0.67	-
NR/PAA20	80 : 20	–	6.0	1.50	-
NR/PAA30	70 : 30	–	6.0	2.57	-
MM10	90 : 10	90 : 10	6.0	0.67	0.74
MM20	90 : 10	80 : 20	6.0	0.67	1.67
MM30	90 : 10	70 : 30	6.0	0.67	2.86

zeolite-PAA mixture followed by the addition of the EG crosslinker. The amount of crosslinker was 1 mole EG per 2 moles of acrylic acid unit. The mixture of NR-zeolite-PAA with crosslinker was then heated to 70°C and maintained at this temperature for 3 h under constant stirring. To prepare the membranes, the NR-zeolite-PAA mixture was cast on a porous nylon support (Osmonics Magna) and dried at 70°C for 48 h in the oven where PAA was allowed to crosslink in the presence of NR. The membrane thickness without the support was about 170 ±10 μm measured at five different points using a micrometer (Mitutoyo). For the NR-*blend*-PAA membranes (NR/PAA), the preparation was the same except that the zeolite was not added to PAA solution only NR latex was blended with PAA solution. The weight compositions of materials for the membrane preparation are given in Table I.

Membrane characterizations

Thermogravimetric analysis (TGA) of the membranes was conducted on PerkinElmer Pyris Diamond TG/DTA analyzer under a nitrogen atmosphere with a heating rate of 10°C/min and temperature up to 600°C. The surface and cross-sectional of MMMs were examined using scanning electron microscopy (SEM) LEO 1450 VP. The samples were coated with a conductive layer of sputtered gold.

Membrane swelling and sorption

Dry membranes were weighted (W_d) and immersed in different concentrations of water–ethanol mixtures. The membranes were left in the liquid solutions for 48 h. The swollen membranes were taken out and blotted with filter paper to remove any excess liquid on the membrane surfaces and then weighted (W_s). The degree of swelling of the membranes was calculated using the following equation:

$$\text{Swelling degree} = \frac{W_s - W_d}{W_d} \quad (1)$$

Immediately after the swelling, a sorption study was carried out as follows. The swollen membrane was placed in a dry flask which connected to a cold trap and a vacuum pump. The flask was heated to 100°C under vacuum to vaporize the liquid retained inside the membrane and the vapor was condensed in the cold trap quenched in liquid nitrogen. The condensed liquid was analyzed with a refractive index detector (Waters RI 2414) and ethanol concentration was determined using the calibration curve constructed from the plot between the compositions of water–ethanol mixtures (vol %) and theirs refractive indices. The water sorption selectivity of a membrane (α_s) is defined as:

$$\alpha_S = \frac{C_W/C_E}{X_W/X_E} \quad (2)$$

where the subscripts W and E refer to water and ethanol, respectively. C and X are volume fractions of water or ethanol in the membrane and the water–ethanol solution, respectively.

Pervaporation

A standard pervaporation process[20] was employed using a custom-made pervaporation module. The effective membrane area was 17.34 cm^2. The pressure on the permeate side was maintained at about 3 mbar using a vacuum pump. Feed temperature was controlled by an oil-bath heater. Permeate vapor was condensed in the cold traps immersed in liquid nitrogen, while the liquid retentate was circulated back to a feed reservoir. Before starting the vacuum pump, the feed solution was flow through a membrane for 2 h. The pervaporation process was then started and operated for 3 h. Afterward the vacuum was terminated and the condensed-permeate was removed from the cold traps and weighed. The composition of the permeate was determined using the calibration curve of the solution compositions versus theirs corresponding refractive indices. The total permeate flux (J) and the water separation factor (α_p) were calculated as follows:

$$J = \frac{W}{A \cdot t} \quad (3)$$

$$\alpha_P = \frac{Y_W/Y_E}{X_W/X_E} \quad (4)$$

where W, A, and t represent the weight of permeate (g), an effective membrane area (m^2), and operating

time (h), respectively. Y and X are volume fractions of water or ethanol in the permeate and the feed, respectively. A permeation flux of each mixture-component was obtained from a product of the total permeation flux with the weight fraction of each component in the permeate.

According to the solution-diffusion mechanism,[21] the permeation flux can be expressed as[22]:

$$J_i = \left(\frac{P_i}{l}\right)\left(x_i\gamma_i p_i^S - y_i p^P\right) \quad (5)$$

where the subscript i stands for water or ethanol. The term P/l is called the permeance where P is the membrane permeability which is a product of the solubility (S) and diffusivity (D) and l is a dry membrane thickness. p^S represents the saturated vapor pressure and was estimated from the Antoine equation.[23] p^P is the permeate-side pressure. x and y are, respectively, mole fractions of the component in feed and permeate. The activity coefficients of feed components γ were determined by the nonrandom two liquid model (NRTL) using Aspen Plus® software. The water selectivity (β) of a membrane is defined as a permeance ratio of water to ethanol.

The temperature dependence of flux and permeance is described in terms of the Arrhenius relationship[24] as expressed in eqs. (6) and (7).

$$J_i = J_{0i}\exp\left(-E_{Ji}/RT\right) \quad (6)$$

$$\frac{P_i}{l} = \frac{P_{0i}}{l}\exp\left(-E_{Pi}/RT\right) \quad (7)$$

where E_J and E_P are the activation energies of flux and permeance, respectively and RT is the thermal energy term. The difference between E_J and E_P is the molar heat of vaporization ΔH_v such that $E_P = E_J - \Delta H_v$.[24]

The diffusion coefficients were also evaluated. If the equilibrium between bulk feed and the upstream surface of a membrane is established, from the Fick's law of diffusion and assuming a linear profile of the concentration along the diffusion length, the diffusion coefficient (D) can be approximated from the following equation:[25]

$$D_i = \frac{J_i l}{C_i} \quad (8)$$

where C is the concentration of each component in feed (g/m^3).

RESULTS AND DICUSSION

Thermogravimetry analysis

The thermogravimetry (TG) curves and their derivative profiles (DTG) of NR/PAA10 membrane and MMMs are displayed in Figure 1. All membranes revealed a three-step weight loss where the first weight loss appeared at 40–150°C followed by the second one at 160–240°C and finally, the major weight loss occurring at 280–400°C. The first weight loss is attributed to loss of absorbed water which is strongly bound to the carboxylic groups of PAA.[26] The second weight loss occurs from the disintegration of crosslink sites of the PAA networks, ester linkages.[12] The major weight loss corresponds to the decomposition of main chains PAA and NR. For MMMs, there were the residues after 480°C which obviously was the embedded-zeolite that does not decompose for temperature up to 600°C.

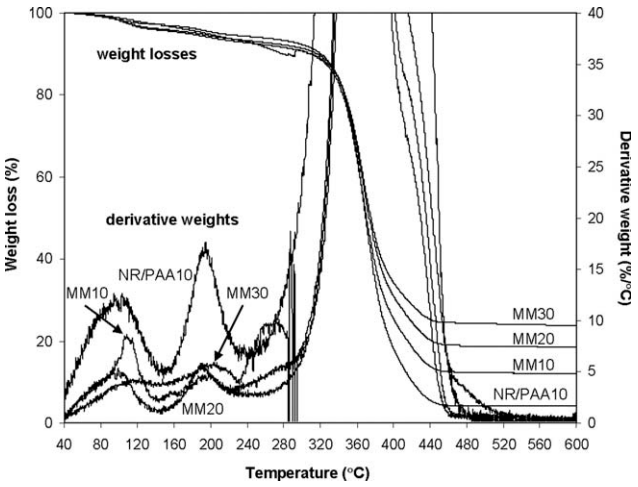

Figure 1 Weight losses and derivative weights of NR/PAA10 and MMMs with 10 (MM10), 20 (MM20), and 30 (MM30) wt % zeolite loading.

Membrane swelling

The swelling behaviors of NR/PAA and MMMs in water–ethanol solutions are demonstrated in Figure 2. Similar swelling patterns were observed in all membranes. The highest degree of swelling was attained in pure water and the swelling declined as the ethanol concentration in the liquid mixtures increased until it reached the threshold at about 70 vol % of ethanol where the membranes became almost no-swelling. Although PAA interacts strongly with water, the presence of ethanol in the liquid mixtures disturbs the interactions of water molecules with the carboxylic acid groups on PAA molecules. Thus, it deters the absorption of water into the membranes and results in a decreased degree of swelling. Moreover, under high ethanol concentrations, the carboxylic groups of PAA are hardly dissociated; therefore the intra- and intermolecular attractions among PAA chains are realized via the H-bonding providing a highly compact network structure. Consequently, the intrusion of ethanol and water

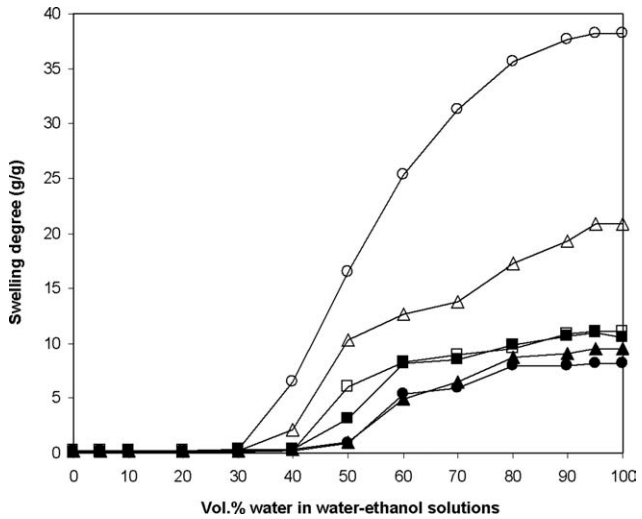

Figure 2 Swelling degrees in water–ethanol mixtures of NR/PAA10 (□), NR/PAA20 (△), NR/PAA30 (○), MM10 (■), MM20 (▲), and MM30 (●) membranes.

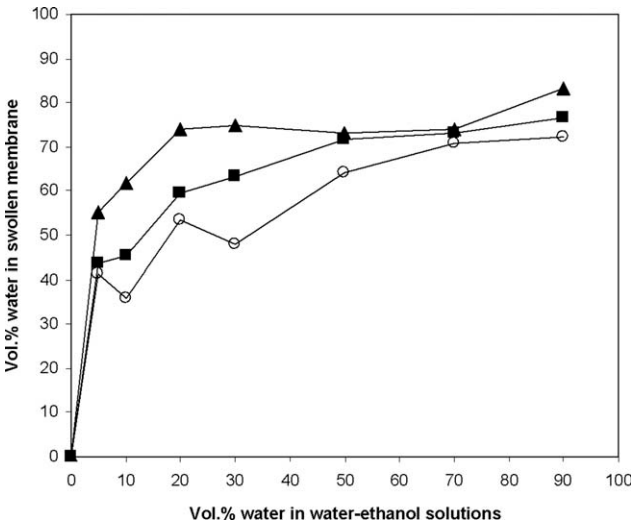

Figure 3 Water sorption isotherms of NR/PAA10 (○), MM10 (■), and MM20 (▲) membranes.

molecules into the membrane structure will be difficult. In contrast, under high water concentrations (more than 30 vol %), the membranes swelled considerably because the –COOH groups on PAA are ionized, producing more -COO^- that generates the repulsion among PAA ionized-chains resulting in the expanded PAA networks. These ionized groups also interact strongly with water molecules via the ion-dipole interaction which promotes the penetration of water molecules into the membranes.[3]

From Figure 2, an effectiveness of NR in suppressing the membrane swelling is evident. By increasing the amount of NR in the NR/PAA membranes, the number of water-attractive carboxylic groups is reduced rendering the membranes more hydrophobic. To a lesser extent, the zeolite can also limit the swelling of the membranes since its presence places a restriction on polymeric chain movements and acts as a physical crosslink for the surrounding polymer molecules.[27]

Membrane sorption

The water sorption isotherms of NR/PAA10 and MMMs are presented in Figure 3. All membranes show a type I adsorption isotherm, implying that the membranes are highly hydrophilic.[28] Besides the interaction with PAA, water molecules can be adsorbed on the zeolite 4A through the interactions with the terminating silanol groups (Si—OH) and the Na^+ extra-framework cations.[28] Therefore the number of water-active sites increased as the zeolite loading increased. This resulted in the isotherms becoming steeper and reaching the saturations at lower water concentrations of water–ethanol mixtures. It could expect that the zeolite particles are more likely be surrounded by PAA networks through the interaction between –COOH pendant groups of PAA and the silanol groups on the zeolite surface. These PAA-surrounded zeolites will appear as the hydrophilic dispersed-phase in the hydrophobic NR matrix.

The ability of membranes to preferentially absorb water over ethanol was evaluated in term of the water sorption selectivity (α_S). The α_S of the membranes at different concentrations of water–ethanol mixtures is presented in Figure 4. Noticeably, there were two distinct regions in which, for a water concentration of less than 70 vol %, the membranes were able to selectively absorb water with the capability of absorption depending on the amount of zeolite. As the water concentrations greater than 70 vol %, the membranes entered the nonselective region where the α_S values were low ($\sim$ 1.0) and nearly inseparable. This is because the polymeric networks are expanded, which is induced by the

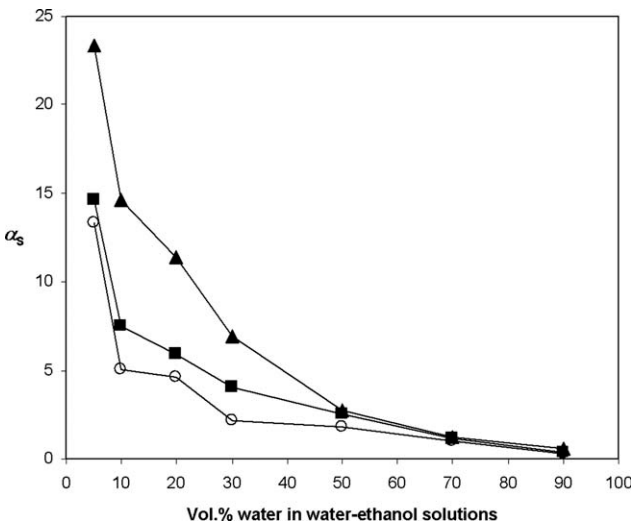

Figure 4 Water sorption selectivities (α_S) of NR/PAA10 (○), MM10 (■) and MM20 (▲) membranes.

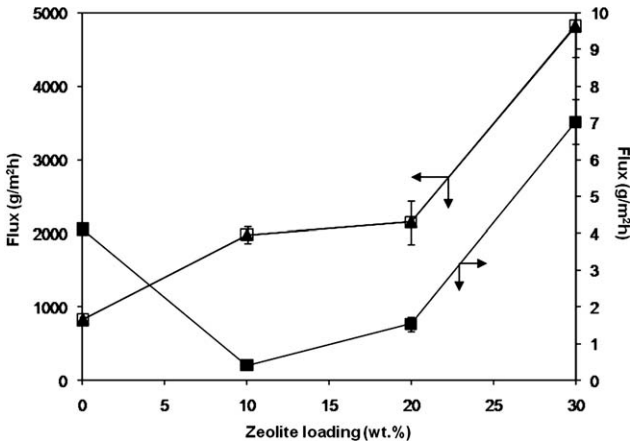

Figure 5 Effect of zeolite loading (wt %) in MMMs on total fluxes (▲), water fluxes (□) and ethanol fluxes (■) for the pervaporation of water–ethanol mixtures; feed water concentration was 10 vol % and feed temperature was 30°C.

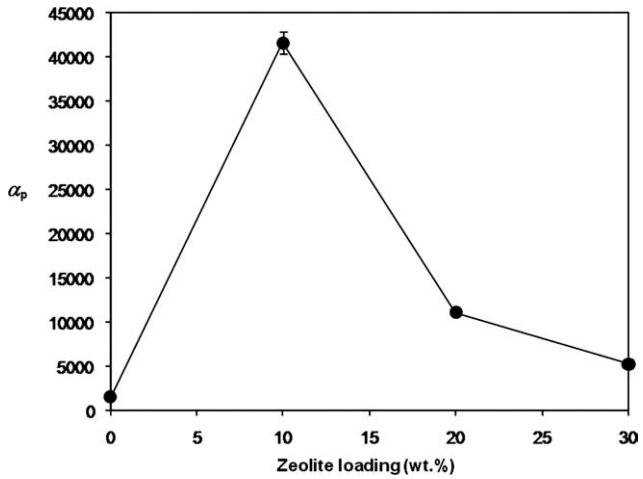

Figure 6 Effect of zeolite loading (wt %) in MMMs on α_P (●) for the pervaporation of water–ethanol mixtures; feed water concentration was 10 vol % and feed temperature was 30°C.

PAA ionized-chains under high water concentration, permitting ethanol and water molecules to transport impartially into the membranes.[29,30]

Pervaporation

Effect of zeolite loading

The separation performance in terms of flux and separation factor (α_P) of the MMMs is demonstrated in Figures 5 and 6, respectively, for the pervaporation dehydration of a water–ethanol mixture with a 10 vol % water in the feed. It is obvious that the membranes are highly water-selective since the water flux contributed almost entirely to the total flux with approximately three orders of magnitude greater than the ethanol flux. As the zeolite loading increased, the total flux was profoundly improved which was given by the enhancement of water flux.

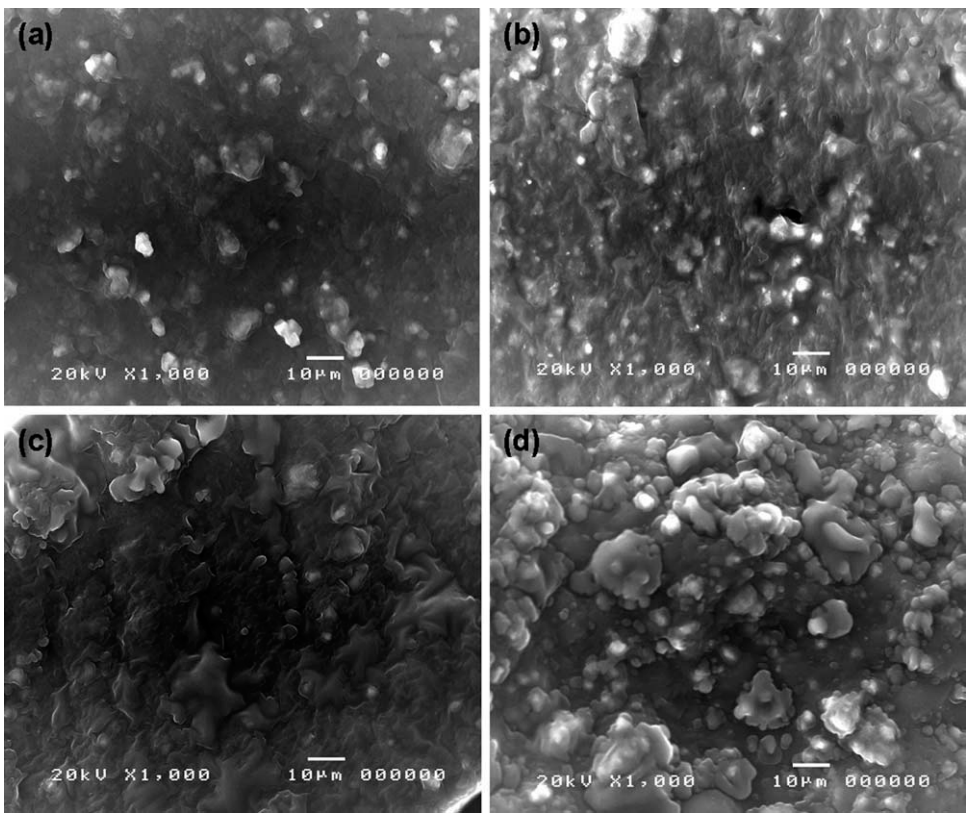

Figure 7 SEM images of surface-MM10 (a), surface-MM30 (b), crosssection-MM10 (c), and crosssection-MM30 (d).

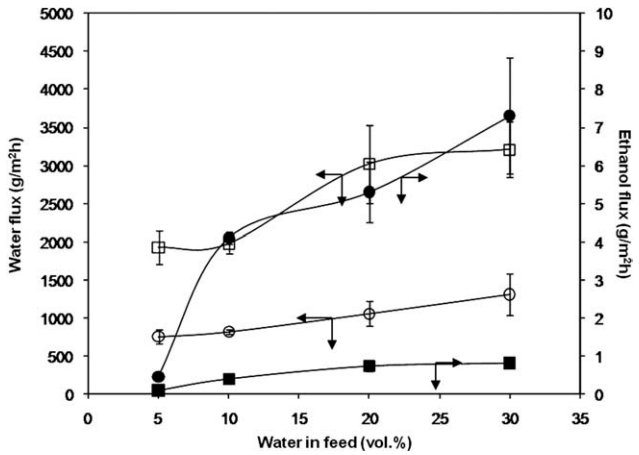

Figure 8 Effect of water concentration in water–ethanol feed mixtures on water (open symbols) and ethanol fluxes (close symbols) of NR/PAA10 (○,●) and MM10 (□,■) membranes; feed temperature was 30°C.

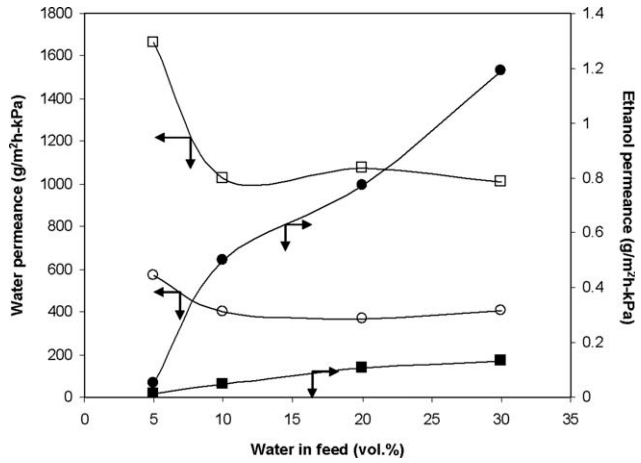

Figure 9 Effect of water concentration in water–ethanol feed mixtures on water (open symbols) and ethanol (close symbols) permeances of NR/PAA10 (○,●) and MM10 (□,■) membranes; feed temperature was 30°C.

In the dense NR/PAA membrane that is composed of hydrophilic and hydrophobic phases, only the hydrophilic PAA channels allow a permeation of water. When zeolite 4A is incorporated with the dense membrane, additional pathways for water diffusion are created through the zeolite's porous structure with the result of a higher permeation of water. Furthermore the molecular sieving effect of zeolite 4A was evident as the flux of ethanol was reduced upon the addition of the zeolite.

If zeolite particles are well distributed in the NR/PAA matrix with a perfect zeolite–polymer interfacial adhesion, it is more likely to observe a decrease of ethanol flux as the zeolite loading increases. However, the results showed the opposite despite a decrease in ethanol flux upon introduction of the zeolite. Accordingly, the membranes encountered a decline of the water selectivity as shown in Figure 6. For MMMs, defects such as the interfacial leak-flow arising from a poor adhesion at interfaces [31] and the interstitial cavities generated by aggregation of zeolite particles in polymer matrix[32] possibly exist. Apart from the swelling effect, both defects in the MMM causes enhanced permeation with reduced selectivity.[33] As revealed by SEM images in Figure 7, the MMM with higher zeolite loading possessed more aggregates than that of a membrane with less zeolite loading, indicating that the aggregate cavities contribute to the deterioration of membrane selectivity.

Effect of feed composition

Figure 8 presents the fluxes of water and ethanol through NR/PAA10 and MM10 membranes when the pervaporation was carried out at different water concentrations of feed water–ethanol mixtures. As the feed water concentration increased, an increase in both water and ethanol fluxes was apparent with significantly higher flux of water than that of ethanol. When a concentration of preferential- permeating specie in feed is high, it is commonly explained that membranes experience an extensive swelling that leads to expanded polymeric networks with a consequence of increased permeation of less-permeating component.[22,34-36]

Unlike the permeation flux, the permeance reveals intrinsic separation property of the membranes because the influence of driving force across the membrane, that is the partial pressure difference, is not accounted for. As shown in Figure 9, the water permeances of both membranes decreased when the water concentration changed from 5 to 10 vol % and were then almost constant for higher water concentration. On the contrary, the ethanol permeances

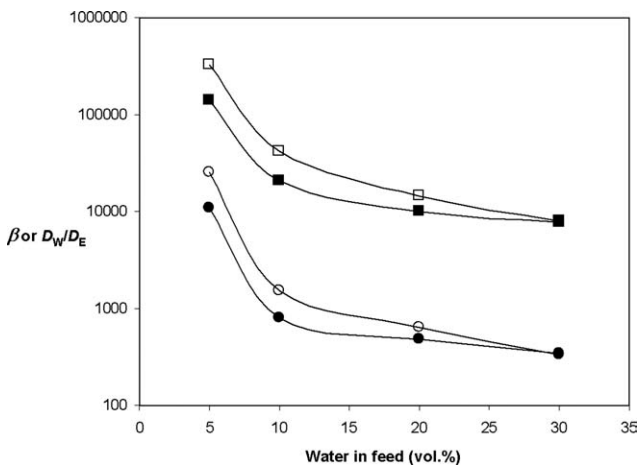

Figure 10 Effect of water concentration in water–ethanol feed mixtures on β (close symbols) and D_W/D_E (open symbols) of NR/PAA10 (○,●) and MM10 (□,■) membranes; feed temperature was 30°C.

TABLE II
Effect of Feed Temperature on the Separation Performance of NR/PAA10 and MM10 Membranes

	Flux (g/m^{2}h)			Permeance (g/m^{2}h-kPa)		
Feed temperature (°C)	Water	Ethanol	α_P	Water	Ethanol	β
NR/PAA10 membrane						
30	760	0.470	28410	625.7	0.051	12,190
40	2067	10.36	3496	974.1	0.659	1,478
50	2347	12.71	3216	659.1	0.491	1,341
60	2414	13.25	3156	418.7	0.322	1,300
70	3472	19.64	3049	384.3	0.309	1,242
MM10 membrane						
30	1927	0.111	319900	1637	0.012	136,321
40	3019	0.225	244847	1468	0.014	102,802
50	3075	0.281	198505	891	0.011	82,233
60	3117	0.337	167233	558	0.008	68,433
70	3282	0.537	109900	375	0.008	44,468

increased with feed water concentration. As a result, the water selectivity (β) was reduced as evidenced in Figure 10. The results of permeances and selectivity suggest that increasing the feed water concentration has a detrimental effect on the separation performance of both dense NR/PAA10 and MM10 membranes. It also implies that as water content in feed increases, the penetration of ethanol molecules through the membranes is promoted with the aid of water molecules. This is clearly observed in Figure 10 when the ratio of water diffusion coefficient to that of ethanol (D_W/D_E) is plotted with feed water concentrations. Despite the significantly high D_W compared with D_E, their ratios declined rapidly with increasing water content in the feed which confirms that the diffusion of ethanol is enhanced as more water is presented in the membranes.

Effect of feed temperature

In pervaporation, one of the important parameters affecting the separation performance of the membranes is feed temperature. Table II summarizes the separation performance of NR/PAA10 and MM10 membranes when the pervaporation was performed at different feed temperature for 5 vol % feed water concentration. Both fluxes of water and ethanol increased as the feed temperature was raised from 30 to 70°C. Traditionally, it is explained that under thermal agitation, the polymer segments are more mobile and thus facilitate a transport of the permeants through a membrane.[22,35,37,38] Nevertheless the thermal-induced mobility of polymeric chains is not the only cause of the flux enhancement. The water permeances, instead, was found to decline as feed temperature rose whereas the ethanol permeance was less affected. Since the flux is dependent on the partial pressure difference which is a function of two temperature-dependent factors: γ and p^S and because p^S is much more sensitive to a change in feed temperature than γ, it is conceivable that the flux is enhanced as feed temperature is elevated because of an increase in p^S.[22]

With an increasing in ethanol permeation at higher feed temperature, a decrease of water selectivity was encountered as observed in Table II. Despite its decrement with the temperature, it is clear that the water selectivity was significantly improved upon incorporating of zeolite 4A with the NR/PAA membrane.

From the results of water and ethanol permeations at different feed temperatures, the Arrhenius plots were constructed as shown in Figures 11 and 12, respectively. It is evident that all the plots were reasonably linear suggesting that the temperature dependence of water and ethanol permeations through NR/PAA10 and MM10 membranes obeyed the Arrhenius relationship. Sequentially, the activation energies were estimated and are summarized in Table III. For all membranes, the activation energies of

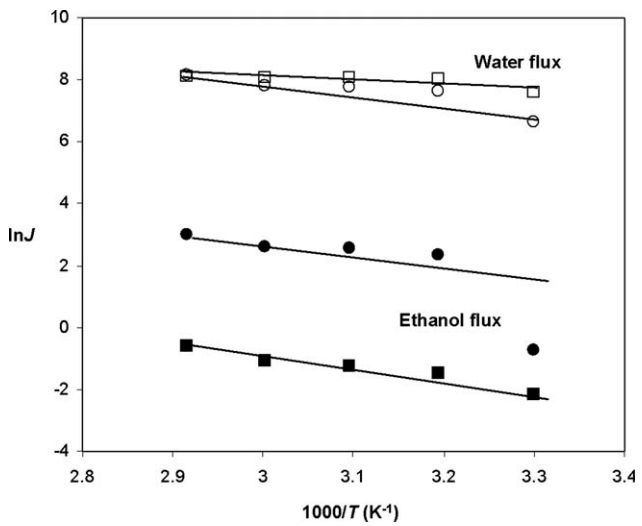

Figure 11 Arrhenius plots of water and ethanol fluxes through NR/PAA10 (○,●) and MM10 (□,■) membranes under feed water concentration of 5 vol %.

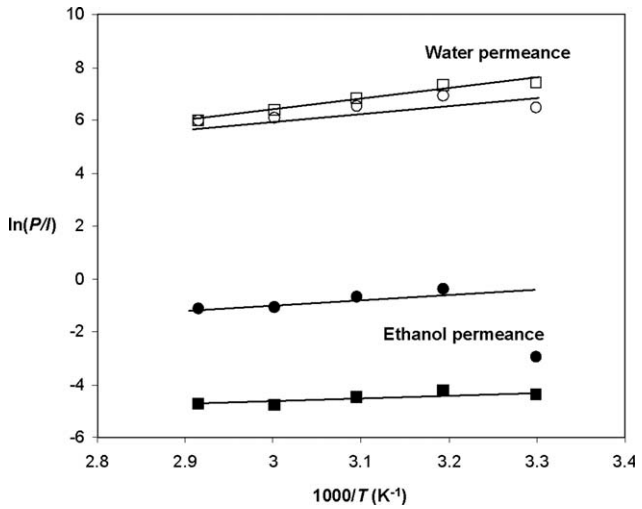

Figure 12 Arrhenius plots of water and ethanol permeances through NR/PAA10 (○,●) and MM10 (□,■) membranes under feed water concentration of 5 vol %.

flux were positive with the activation energies of water flux (E_{JW}) being lower than those of the ethanol flux (E_{JE}). This means that water molecules experience a less energy barrier in permeating through the membranes compared with the transport of ethanol. Furthermore the addition of zeolite 4A resulted in decreasing of E_{JW}, while E_{JE} showed the opposite, suggesting that the presence of zeolite provides less resistance paths for water molecules but gives more resistance for ethanol molecules. Table III also shows the estimated ΔH_v, which, for all membranes possessed almost the same values of 43.3 kJ/mol for water and 41.7 kJ/mol for ethanol. These ΔH_v values were closed to those reported previously.[14]

The activation energies of both water (E_{PW}) and ethanol (E_{PE}) permeances showed negative values which could be expected from the declines of water and ethanol permeances with temperature. According to the solution-diffusion model of permeation, membrane permeability (P) depends upon the diffusivity (D) and solubility (S) of permeant with a membrane, i.e., $P = D \times S$. In the case of temperature dependence, if P follows the Arrhenius relationship, D and S are expressed by the Arrhenius type of relation as well, where the activation energy of permeability (E_P) is a combination of the activation energy of diffusion (E_D) and the enthalpy of sorption (ΔH_S) of permeant in a membrane such that $E_P = E_D + \Delta H_S$.[24] The diffusivities of water and ethanol were approximated by eq. (8) and the Arrhenius plots of the diffusivity were constructed accordingly as shown in Figure 13. Evidently, the negative slopes were obtained giving the positive values of activation energy for diffusivity of water (E_{DW}) and ethanol (E_{DE}), as reported in Table III. This indicates that raising the temperature promotes the diffusivity of the permeants and after the zeolite is incorporated, E_{DW} became lower in contrast

TABLE III
Estimated Parameters Obtained from the Arrhenius Plots of the Permeations of Water and Ethanol through NR/PAA10 and MM10 Membranes

Parameters (kJ/mol)	NR/PAA10		MM10	
	Water	Ethanol	Water	Ethanol
E_J	14.01	17.38	11.71	30.87
E_P	−29.10	−24.14	−31.67	−10.87
ΔH_V	43.11	41.52	43.37	41.74
E_D	14.47	18.32	10.09	31.77
ΔH_S	−43.56	−42.45	−41.76	−42.63

to E_{DE}, which indicates that a well-defined porous structure of zeolite 4A enhances the diffusivity of water molecules but depreciates the ethanol diffusion. Since E_D was positive, the negative E_{PW} and E_{PE} suggest the exothermic sorption processes of both water and ethanol in the membranes. Although zeolite 4A provides additional favorable-sorption sites for water molecules,[39] ΔH_S values of water and ethanol sorption were similar regardless of the presence of zeolite 4A indicating the prevailing effect of PAA over the zeolite in the water and ethanol sorption.

Comparison of pervaporation (PV) performance of MMMs

Table IV compares the pervaporation performance of the MMMs in this work with others reported in the literatures for the dehydration of water–ethanol mixtures. Our developed membranes possess relatively high flux with superior separation factor, as high as 320,000, particularly at 5 vol % feed water concentration. Promisingly, a combination of hydrophobic-hydrophilic blend membrane of NR/PAA with the zeolite 4A would yield

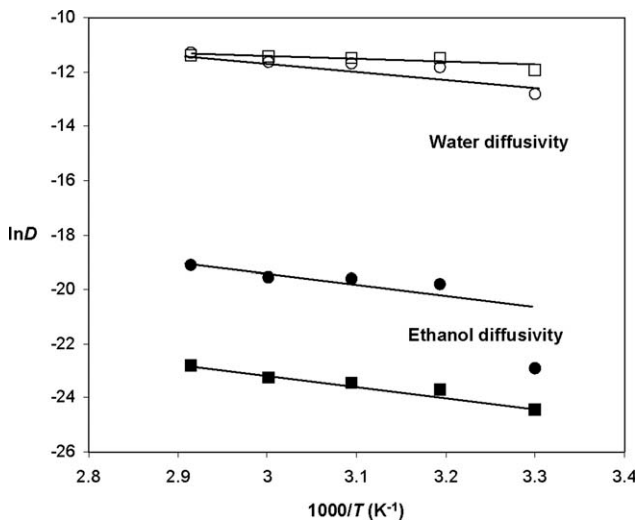

Figure 13 Arrhenius plots of water and ethanol diffusivities through NR/PAA10 (○,●) and MM10 (□,■) membranes under feed water concentration of 5 vol %.

TABLE IV
Comparison of PV Performance of MMMs Reported in the Literatures for the Dehydration of Water–Ethanol Mixtures

Membrane	Particle loading (wt %)	Feed water content	Feed temperature (°C)	Flux (g/m^2h)	α_P	Reference
PVA-4A	20	23.6 wt %	60	936	710	14
PVA-KA	20	20 wt %	80	507	963	15
PSf[a]-4A	44	10 wt %	25	175	351	18
PSf-nano $Fe(CO)_5$	8	10 wt %	25	>500	50,000	40
NaAlg[b]-Beta	10	10 wt %	30	132	1,598	41
NR/PVA-4A	10	10 vol %	30	2281	940	42
NR/PAA-4A	10	5 vol %	30	1927	320,000	This study
NR/PAA-4A	10	10 vol %	30	1977	41,600	This study

[a] PSf, polysulfone.
[b] NaAlg, sodium algenate.

water-selective membranes with a marked improvement in water separation performance.

CONCLUSIONS

The water-selective MMMs were developed from natural rubber (NR) blended with poly(acrylic acid) (PAA) and filled with zeolite 4A. While PAA promotes the hydrophilicity of the membranes, thus improving the water absorption, NR renders the membranes more hydrophobic and limits the swelling of the membranes. Zeolite 4A was incorporated to enhance the water permeation and improve the water selectivity of the membranes. With the incorporated-zeolite behaving like a physical crosslink of the surrounding polymers, the MMMs develop less membrane swelling compared with NR/PAA membranes. The water sorption selectivity was determined as a function of water concentration in the water–ethanol mixtures. The results indicated two regions: for water concentrations less than 70 vol.%, the sorption selectivity increased with the zeolite loading and PAA content and for water concentrations greater than 70 vol.%, the membranes enter the region of nonselective sorption. The dehydration of water–ethanol mixtures was performed by the pervaporation and the results revealed that the water flux was almost three-order of magnitude greater than the flux of ethanol, indicating that the developed membranes were highly water-selective. Also, by incorporating the zeolite 4A, the flux and separation factor were improved when compared with NR/PAA membranes. Increasing the water content in the water–ethanol feed mixtures caused not only the water flux but also the ethanol flux to increase leading to a decline in water selectivity. Raising feed temperature resulted in increases of both water and ethanol fluxes with a decrease of water selectivity. The water permeance, however, declined as feed water concentration as well as feed temperature increased, suggesting the pronounced effect of the partial pressure difference across a membrane on the water flux enhancement. The partial pressure difference, on the other hand, was less influential on the ethanol permeance. The Arrhenius plots of the permeations were constructed, giving the activation energies for water and ethanol permeation through the membranes. The activation energies of water permeation were lower than those of ethanol permeation suggesting that water molecules are transporting through the membranes with less restriction compared with the transport of ethanol molecules.

References

1. Standard specification for denatured fuel ethanol for blending with gasolines for use as automotive spark-ignition engine fuel, ASTM International, ASTM D4806-09.
2. Chapman, P. D.; Oliveira, T.; Livingston, A. G.; Li, K. J Membr Sci 2008, 318, 5.
3. Semenova, S. I.; Ohya, H.; Soontarapa, K. Desalination 1997, 110, 251.
4. Choi, H. S.; Hino, T.; Shibata, M.; Negishi, Y.; Ohya, H. J Membr Sci 1992, 72, 259.
5. Ohya, H.; Shibata, M.; Negishi, Y.; Guo, Q. H.; Choi, H. S. J Membr Sci 1994, 90, 91.
6. Lee, K. R.; Teng, M. Y.; Lee, H. H.; Lai, J. Y. J Membr Sci 2000, 164, 13.
7. Lee, Y. M.; Nam, S. Y.; Ha, S. Y. J Membr Sci 1994, 159, 41.
8. Meier-Haack, J.; Lenk, W.; Lehmann, D.; Lunkwitz, K. J Membr Sci 2001, 184, 233.
9. Zhang, G.; Gu, W.; Ji, S.; Liu, Z.; Peng, Y.; Wang, Z. J Membr Sci 2006, 280, 727.
10. Adoor, S. G.; Manjeshwar, L. S.; Kumar Naidu, B. V.; Sairam, M.; Aminabhavi, T. M. J Membr Sci 2006, 280, 594.
11. Sridhar, S.; Smitha, B.; Reddy, A. A. Colloid Surface A 2006, 280, 95.
12. Amnuaypanich, S.; Kongchana, N. J Appl Polym Sci 2009, 114, 3501.
13. Hyder, M. N.; Huang, R. Y. M.; Chen, P. J Membr Sci 2006, 283, 281.
14. Huang, Z.; Guan, H.; Tan, W.; Qiao, X. Y.; Kulprathipanja, S. J Membr Sci 2006, 276, 260.
15. Guan, H. M.; Chung, T. S.; Huang, Z.; Chng, M. L.; Kulprathipanja, S. J Membr Sci 2006, 268, 113.
16. Clarizia, G.; Algieri, C.; Drioli, E. Polymer 2004, 45, 5671.
17. Qiao, X.; Chung, T.; Rajagopalan, R. Chem Eng Sci 2006, 61, 6816.
18. Fu, Y. J.; Hu, C. C.; Lee, K. R.; Lai, J. Y. Desalination 2006, 193, 119.

19. Bowen, T. C.; Noble, R. D.; Falconer, J. L. J Membr Sci 2004, 245, 1.
20. Mulder, M. Basic Principles of Membrane Technology; Kluwer: the Netherlands, 1991.
21. Wijmans, J. G.; Baker, R. W. J Membr Sci 1995, 107, 1.
22. Guo, W. F.; Chung, T. S.; Matsuura, T. J Membr Sci 2004, 245, 199.
23. Foust, A. S.; Wenzel, L. A.; Clump, C. W.; Maus, L.; Andersen, L. B. Principles of Unit Operations, 2nd ed.; Wiley: New York, 1980.
24. Feng, X.; Huang, R. Y. M. J Membr Sci 1996, 118, 127.
25. Kusumocahyo, S. P.; Sudoh, M. J Membr Sci 1999, 161, 77.
26. Kim, D. S.; Park, H. B.; Rhim, J. W.; Lee, Y. M. J Membr Sci 2004, 240, 37.
27. Moore, T. T.; Mahajan, R.; Vu, D. Q.; Koros, W. J. AIChE J 2004, 50, 311.
28. Ng, E. P.; Mintova, S. Micropor Mesopor Mater 2008, 114, 1.
29. Devi, D. A.; Smitha, B.; Sridhar, S.; Aminabhavi, T. M. Sep Purif Technol 2006, 51, 104.
30. Guo, R.; Hu, C.; Li, B.; Jiang, Z. J Membr Sci 2007, 289, 191.
31. Hillock, A. M. W.; Miller, S. J.; Koros, W. J. J Membr Sci 2008, 314, 193.
32. De Sitter, K.; Winberg, P.; D'Haen, J.; Dotremont, C.; Leysen, R.; Martens, J. A.; Mullens, S.; Maurer, F. H. J.; Vankelecom, I. F. J. J Membr Sci 2006, 278, 83.
33. Cong, H.; Radosz, M.; Towler, B. F.; Shen, Y. Sep Purif Technol 2007, 55, 281.
34. Chen, X.; Yang, H.; Gu, Z.; Shao, Z. J Appl Polym Sci 2001, 79, 1144.
35. Adoor, S. G.; Prathab, B.; Manjeshwar, L. S.; Aminabhavi, T. M. Polymer 2007, 48, 5417.
36. Wang, L.; Li, J.; Lee, Y.; Chen, C. Chem Eng J 2009, 146, 71.
37. Hsueh, C. L.; Kuo, J. F.; Huang, Y. H.; Wang, C C.; Chen, C. Y. Sep Purif Technol 2005, 41, 39.
38. Liu, X.; Sun, Y.; Deng, X. J Membr Sci 2008, 325, 192.
39. Kariduraganavar, M. Y.; Varghese, J. G.; Choudhari, S. K.; Olley, R. H. Ind Eng Chem Res 2009, 48, 4002.
40. Chen, S. H.; Liou, R. M.; Lai, C. L.; Hung, M. Y.; Tsai, M. H.; Huang, S. L. Desalination 2008, 234, 221.
41. Adoor, S. G.; Manjeshwar, L. S.; Bhat, S. D.; Aminabhavi, T. M. J Membr Sci 2008, 318, 233.
42. Amnuaypanich, S.; Patthana, J.; Phinyocheep, P. Chem Eng Sci 2009, 64, 4908.